Joint electric vehicle routing and battery health management integrating an explicit state of charge model

Pedro Dias Longhitano, Christophe Bérenguer, Benjamin Echard

Highlights

Joint Electric Vehicle Routing and Battery Health Management Integrating an Explicit State of Charge Model

Pedro Dias Longhitano, Christophe Bérenguer, Benjamin Echard

- A new EVRP formulation that includes battery degradation and speed limitations
- Realistic SoH and SoC models that can be included in optimization problems
- A method to estimate the battery degradation after performing missions
- A genetic programming algorithm to solve the EVRPs
- Numerical experiments to validate the proposed methodology

Joint Electric Vehicle Routing and Battery Health Management Integrating an Explicit State of Charge Model

Pedro Dias Longhitano[a,b], Christophe Bérenguer[b], Benjamin Echard[a]

[a] *Volvo Trucks, 1 Av. Henri Germain, 69806 Saint-Priest, France*
[b] *Univ. Grenoble Alpes, CNRS, Grenoble INP, GIPSA-lab, 38000 Grenoble, France*

Abstract

Although fleet management has been extensively explored in transportation science, the rise of electromobility imposes several scientific challenges and opportunities. So far, few attempts were made to include battery degradation in the Electric Vehicle Routing Problem (EVRP). To do it realistically, it is necessary to model State of Charge (SoC), however most versions of routing problems use oversimplified SoC models or consider only energy consumption which leads to less robust solutions overall. In this work, a method for estimating battery degradation, which relies on a realistic SoC model is presented and incorporated into a new version of the electric vehicle routing problem. In this version, not only battery degradation is integrated, but also the possibility of limiting different vehicle parameters, such as maximum vehicle speed and acceleration. Due to the extra computational complexity related to the SoC and degradation models, a genetic algorithm capable of solving the aforementioned extended EVRP is presented. Finally, through different numerical experiments, the advantages of the proposed methodology are shown.

Keywords: Battery health management, degradation modelling, electric vehicle routing, multi-objective optimization

Email addresses: pedro.dias.longhitano@volvo.com (Pedro Dias Longhitano), Christophe.Berenguer@grenoble-inp.fr (Christophe Bérenguer), benjamin.echard.2@volvo.com (Benjamin Echard)

Preprint

Table 1: Variables glossary

SoH	State of Health
$SoC(t)$	State of Charge
SoH_0	SoH before performing a mission plan
$Q(t)$	battery capacity
Q_0	battery nominal capacity
x_{ijz}	routes decision variables
y_{ijz}	arrival time decision variables
w_{ijz}	vehicle payload decision variables
f_{iz}	recharge time decision variables
v_{max_z}	vehicle maximum speed decision variables
a_{max_z}	vehicle maximum acceleration decision variables
H	maximum allowed vehicle payload
m	vehicle mass
ρ_{air}	air density
V_{OC}	open-circuit voltage
C_r	rolling resistance coefficient
C_w	drag coefficient
A	vehicle frontal area
α	road inclination
len	road link length
v_{road}^{max}	road link maximum allowed speed
$a_{centripetal}$	vehicle maximum centripetal acceleration
v_{tgt}	vehicle target speed
e_{ijz}	consumed energy
h_i	vehicle mass variation
SoC_{crit}	critical SoC limit
t_{ij}	displacement duration
l_j	mission deadline

1. Introduction

Historically, internal combustion engine vehicles have been the norm of transportation. However, to attenuate global warming, different actions to popularize Electric Vehicles (EV's) have been taken. In this new paradigm, the importance of understanding and improving battery lifetime has important economic consequences since this component accounts for around 35% [29] to 50% [5] of the total vehicle cost.

Battery lifetime management has also environmental consequences and is a main concern of several global players. For instance, in the communication of the European Green Deal [10], the importance of ensuring "a safe, circular and sustainable battery value chain for all batteries [...] to supply the growing market of electric vehicles" is emphasized.

Since vehicle usage has a direct influence on battery lifetime, incorporating battery degradation on vehicle decision-making problems can lead to different insights and solutions that extend lifetime [32, 46, 44, 34, 16, 26]. However, most of the degradation models used are incapable of accounting for different driving conditions and degradation induced while driving.

Furthermore, to achieve practical degradation-aware decision-making, optimization models must realistically describe the State of Health (SoH) of the battery, which in turn depends on realistic State of Charge (SoC) models[33]. However, most SoC models considered thus far in such decision-making problems are oversimplified.

Additionally, new technologies allow for different decisions to be considered. For example, the impact on degradation of restricting the vehicle speed and its acceleration, or of partially recharging the battery, remains to be explored.

In our work, we propose an optimization model that leverages SoH estimation based on realistic SoC modeling and is integrated into a new version of the Electric Vehicle Routing Problem (EVRP) that accounts for partial charging, speed and acceleration limitations and also for battery degradation. Due to its computational complexity, a genetic algorithm is used to solve it.

Therefore, the main contributions of this paper can be summarized as follows:

- The formalization of the electric vehicle routing problem with degradation and vehicle parameters (EVRP-DVP). It includes battery degradation modeling, partial charging, maximum speed limitation and maximum acceleration limitation.
- A SoH estimation method that relies on realistic SoC modeling and can be included in optimization problems.
- A method to estimate the battery degradation after performing a set of missions.
- Numerical experiments to validate the proposed methodology.

Accordingly, this paper is structured as follows: Section 2 promotes a bibliography review that places our contribution according to the state-of-art. Section 3 formalizes the optimization problem while Section 4 presents all the necessary physical models. The genetic algorithm used to solve it are presented in Section 5. Section 6 provides numerical results and finally, Section 7 concludes the paper.

2. Bibliography Review

This section reviews both degradation (SoH) and SoC models commonly used in transportation applications.

2.1. Battery Degradation in vehicle applications

Battery SoH can be defined as follows [7]:

$$SoH(t) = \frac{Q(t)}{Q_0} \tag{1}$$

where $Q(t)$ is the battery capacity at instant t and Q_0 is its initial capacity. The SoH decreases until reaching a critical threshold after which the battery must be replaced.

Battery degradation is a complex phenomenon that can occur due to different mechanisms. Among them are the expansion of the Solid Electrolyte Interphase, current collector corrosion, binder and electrolyte decomposition, lithium platting and particle fracture [7, 33, 31]. Some degradation models are directly based on those phenomena and are usually referred to as physical-based models. However, for most vehicle decision-making problems, they are impractical due to their complexity and the difficulty to include them in optimization models related to vehicle exploitation [33].

Black-box models (or data-driven) [41, 4, 40, 45, 21, 22] use battery SoH (or capacity) data to feed algorithms that predict capacity evolution or failure time. The main drawback of this approach is the fact that it relies on large amounts of data, which is rarely available for real vehicle applications where usage conditions can widely vary.

The most suitable models for vehicle decision-making problems are the semi-empirical models because they combine data and theoretical principles. They require less data than a pure black-box approach and are also easier to include in EVRPs than physical-based models since they do not directly describe chemical reactions. Instead, they correlate degradation with stress factors that can be connected to vehicle usage [33]. Some of the most common stress factors are:

- **Mean SoC (mSoC):** defined as the average value of $SoC(t)$. Operating in high mSoc values accelerates degradation mechanisms in the negative electrode [7].
- **Depth of Discharge (DoD):** defined as the amplitude of SoC variation in a discharge cycle. Higher DoD often lead to accelerated capacity fade [7].
- **C-rate:** defined as the rate in which the battery is discharged or charged. It can be estimated through the SoC variation rate. Operating on specific values of C-rate is known to accelerate degradation.

For those reasons, such models are commonly employed in degradation-aware

decision-making problems [44, 16, 34, 46, 32]. However, most of the used degradation models present limitations. They are either too simplistic, or do not account for degradation caused by driving cycles. They are also incapable of considering the effects of opportunistic charges (*i.e.* SoC that is recuperated when braking or driving downhill) and often neglect some important stress factors.

One alternative is to use models based on SoC cycle decomposition, such as [43]. Those models consider that the SoC history can be expressed as a combination of simpler cycles, usually obtained through the Rainflow-Counting algorithm [12]. After the decomposition, stress factors can be computed from the identified cycles characteristics and therefore, the capacity fade caused by each cycle can be calculated.

The main advantage of cycle decomposition models is that usage conditions are not assumed to be static and they can be employed for charge and discharge cycles. Even for batteries types that are more sensible to degradation while charging, cycle decomposition is still useful because it can account for opportunistic charging (charges that occur while driving).

2.2. State of Charge models in the Electric Vehicle Routing Problem

One of the most important problems in transportation science is the Vehicle Routing Problem (VRP) [39, 11]. Several different variations of this problem were studied and, in recent years, the EVRP [13, 24] has become extremely relevant. This version accounts for particularities of electrical vehicles which come from their lower ranges, consumption models and non-neglectable recharge times.

In the classical EVRP formulation, a fleet of EV's, starting in a depot, has to serve a set of customers, minimizing a criterion such as energy consumption or operation time and respecting a set of constraints related to operational conditions and vehicle range (*i.e.* limiting SoC or energy consumption to an acceptable level). The goal of this section is not to extensively review the literature of EVRP's but to analyze recent contributions in terms of models

used to define vehicle range.

Most authors define their constraints in terms of energy consumption. However, this approach is less robust than constraining SoC and can lead to unfeasible routes in some cases [33]. It is also important to highlight that some authors treat SoC and energy variation as synonyms. The implicit assumption is that the terminal battery voltage is constant which may not hold for some battery types and applications.

Some authors do not discuss explicitly how to model either SoC variations or energy consumption but consider it to be known in advance for a given displacement. This approach is used in works such as [23] where authors are interested in the problem of partial charging with non-linear profiles. Similar examples can be found in [30, 17, 15].

In [20], a model for a EVRP that also accounts for battery degradation is proposed. It considers both SoC and energy to be directly proportional to the traveled distance. A large number of works use similar approaches [37, 47, 35, 9]. However, considering energy or SoC to be proportional to the traveled distance can lead to significant errors in urban networks [8].

In [28], energy is estimated assuming that vehicles move with constant speed trough each edge and constant power-train efficiency, not accounting for acceleration effects. Similar energy models can be found in [1, 2, 14, 27].

[6] uses vehicle dynamics equations combined with prior speed profiles to estimate energy consumption. This approach can lead to realistic estimates but knowledge on speed profiles can be restrictive in most scenarios due to the lack of data. Authors consider SoC to vary directly with consumed energy, implying constant terminal voltage.

In [8], a two-step EVRP is solved, in which the energy model is based on road topography, making assumptions on driving cycles and accounting for power-train efficiency. This model is compared with real vehicle data and presents a mean square error close to 12%. In the associated optimization model, constraints related to vehicle range are defined in terms of energy.

To the best of our knowledge, no realistic SoC model has been included in

EVRP's. The importance of considering realistic SoC models is highlighted by [33]. Our contribution in this work is thus to propose and solve a new version of the EVRP, integrating a realistic SoC model: EVRP-DVP, electric vehicle routing problem with degradation and vehicle parameters.

3. Problem Formulation

The EVRP-DVP is a decision making problem that consists on assigning different missions (deliveries) to a fleet vehicles. Each mission has a known deadline and the mission planning is built considering range limitations and minimizing an objective criterion that accounts for degradation and logistic costs.

To formalize the EVRP-DVP as an optimization problem, we consider the graph $G = (N, E)$. Nodes N can be described as $N = C \cup S \cup 0$ where C is the set of clients, S is the set of charging stations and 0 represents the headquarters, where vehicles start and to where they must come back at the end of their missions. The set of vehicles is denoted by Z.

The decision variables are: x_{ijz}, a binary variable that is 1 if vehicle z drives from node i to node j and zero otherwise; w_{ijz}, the payload of vehicle z while going from i to j; y_{ijz} which is the arrival time of vehicle z at node j from node i and f_{iz} which is the time spent by vehicle z on recharge station i. Together, those decision variables define a mission plan and a vehicle configuration.

Decision variables a_{max_z} represent the maximum acceleration of vehicle z; and v_{max_z} the maximum speed of vehicle z. They are vehicle software parameters that can be changed remotely. As a consequence, those parameters will affect the how vehicle speed behaves during displacements. Figure 1 shows the speed of two vehicles with different a_{max_z} and v_{max_z} making the same displacement.

In addition to decision variables, other terms are needed to establish EVRP constraints. H is the maximum vehicle payload, $t_{ij}(v_{max_z}, a_{max_z})$ is the time necessary to go from i to j with v_{max_z} and a_{max_z}, $SoC(t, X_z, v_{max_z}, a_{max_z})$

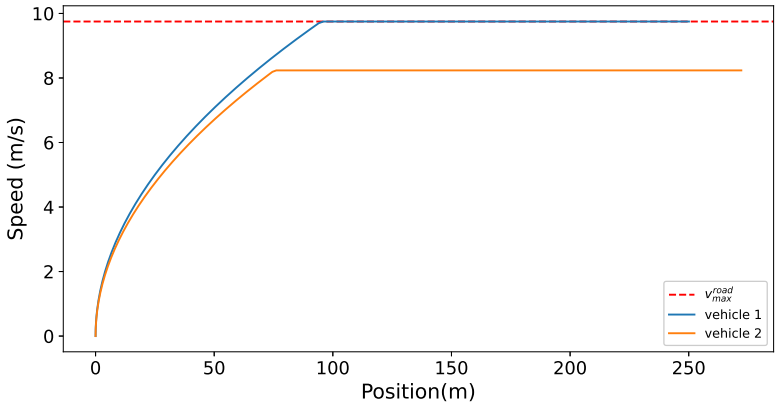

Figure 1: Speed comparison of two vehicles with different a_{max_z} and v_{max_z}. In this case, both a_{max_2} and v_{max_2} are inferior to a_{max_1} and v_{max_1} respectively. As a consequence, vehicle 1 is able to reach nominal while vehicle 2 has its speed limited to 8 m/s.

indicates SoC at instant t for vehicle z, given v_{max_z}, a_{max_z} and a mission plan defined by X_z which denotes the set of x_{ijz} that are equal to 1 for vehicle z, SoC_{crit} that is critical SoC threshold and h_i that is the vehicle mass variation caused making the delivery at node i.

The cost function of the mission plan is composed of three components and depends on the decision variables. It is defined as:

$$C = C_{deg} + C_{energy} + C_{delay} \tag{2}$$

- The degradation cost C_{deg} can be expressed as:

$$C_{deg} = c_{batt} \sum_{z \in Z} \Delta SoH(X_z, v_{max_z}, a_{max_z}) \tag{3}$$

where $\Delta SoH(X_z, v_{max}, a_{max})$ is the variation of the battery SoH of vehicle z after performing the missions defined by X_z with maximum speed v_{max_z}, and maximum acceleration a_{max_z}. The constant c_{batt} is based on the battery cost.

- The energy cost C_{energy} is considered directly proportional to the consumed energy and is described by:

$$C_{energy} = \sum_{z \in Z} c_e \sum_{i \in N} \sum_{j \in N} e_{ijz}(v_{max_z}, a_{max_z}) x_{ijz} \tag{4}$$

  where c_e is a constant related the energy cost, $e_{ijz}(v_{max_z}, a_{max_z}))$ is the energy spent by vehicle z going from i to j with v_{max_z} and a_{max_z}.

- And finally, the delay cost C_{delay} which can be expressed as follows:

$$C_{delay} = \sum_{z \in Z} c_d \sum_{i \in N} \sum_{j \in C} x_{ijz} \max[y_{ijz} - l_j, 0] \tag{5}$$

  where c_d is a constant related to the cost of penalties and l_j is the deadline of client j.

The final optimization problem can then be described as:

$$\min \quad C \tag{6}$$

Subjected to:

$$\sum_{z\in Z}\sum_{j\in C} x_{ijz} = 1 \quad \forall i \in N \tag{7}$$

$$\sum_{j\in N} x_{0jz} = 1 \quad \forall z \in Z \tag{8}$$

$$\sum_{j\in S} x_{ijz} \leq 1 \quad \forall i \in N, \forall z \in Z \tag{9}$$

$$\sum_{j\in N} x_{ijz} - \sum_{j\in N} x_{jiz} = 0 \quad \forall i \in N, \forall z \in Z \tag{10}$$

$$\sum_{z\in Z}\sum_{j\in N} w_{ijz} - \sum_{z\in Z}\sum_{j\in N} w_{jiz} = h_i \quad \forall i \in N \tag{11}$$

$$h_j x_{ijz} \leq w_{ijz} \leq (H - h_i)x_{ijz} \quad \forall i \in N, \forall z \in Z \tag{12}$$

$$y_{0jz} \geq t_{0j}(v_{max_z}, a_{max_z})x_{0jz} \quad \forall i \in C \cup S, \forall z \in Z \tag{13}$$

$$\sum_{z\in Z}\sum_{j\in N} y_{ijz} - \sum_{z\in Z}\sum_{j\in N} y_{jiz} \geq t_{ij}(v_{max_z}, a_{max_z})x_{ijz} \quad \forall i \in C \tag{14}$$

$$\sum_{z\in Z}\sum_{j\in N} y_{ijz} - \sum_{z\in Z}\sum_{j\in N} y_{jiz} \geq t_{ij}(v_{max_z}, a_{max_z})x_{ij} + f_{iz} \quad \forall i \in S \tag{15}$$

$$min \quad SoC(t, X_z, v_{max_z}, a_{max_z}) \geq SoC_{crit} \quad \forall z \in Z, \forall t \tag{16}$$

$$x_{ijz} \in \{0, 1\} \tag{17}$$

$$w_{ijz} \geq 0 \tag{18}$$

$$y_{ijz} \geq 0 \tag{19}$$

$$v_{max_z} \in [v^-_{max}, v^+_{max}] \tag{20}$$

$$a_{max_z} \in [a^-_{max}, a^+_{max}] \tag{21}$$

Inequality (7) ensures that every client is visited once, Constraint (8) guarantees that the number of vehicles used does not exceed the size of the fleet and Constraint (9) limits the number of visits to recharge stations. Constraint (10) ensures that there is one outgoing arc to each incoming arc. Constraint (11) guarantees that, at each delivery, the payload is reduced accordingly since $h_i = 0 \quad \forall i \in S \cup 0$, while (12) ensures that the maximum payload H is respected and also it makes $w_{ijz} = 0$ when $x_{ijz} = 0$. Constraints (13) through (15) describe arrival time evolution, ensuring that the displacement duration is

respected. Constraint (16) imposes the range limitations through SoC, which model is presented in section 4. Constraints (17) through (21) define the proper range of the decision variables. And $a^-_{max}, a^+_{max}, v^-_{max}, v^+_{max}$ are the acceptable limits of a_{max_z} and v_{max_z}, respectively.

The next section presents the models used to compute $\Delta SoH(X_z, v_{max_z}, a_{max_z})$, $e_{ijz}(v_{max_z}, a_{max_z})$ and $SoC_{ijz}(t)$ based on the decisions variables of the problem.

4. SoH and SoC estimation method

To solve the EVRP-DVP in realistic cases, it is necessary to combine several models with road information, such as topology, allowed speeds, etc. In this section, all those models are presented as well as the necessary hypotheses.

4.1. Degradation Model

The term $\Delta SoH(X_z, v_{max}, a_{max})$ in Equation (3) can be computed based on the degradation model presented in [43]. It is based on cycle decomposition as mentioned in Section 2.1.

The cycle decomposition can be obtained by a Rainflow-Counting algorithm, and an example of such a decomposition is illustrated in Figure 2, in which 2 cycles are identified and their amplitude (DoD) and mean (mSoC) are denoted by σ and δ respectively.

The degradation model expresses SoH as:

$$SoH(t) = e^{-f_d(t)} \tag{22}$$

With the damage function f_d defined as:

$$f_d(SoC(t)) = \sum_{i=1}^{n(SoC(t)))} u_i \; S_{\delta_i} \; S_{\sigma_i} \; S_{T_i} \tag{23}$$

where $n(SoC(t))$ is the number of SoC cycles up to time t, u_i is 1 for a full cycle or 0.5 for a partial cycle, S_{δ_i}, S_{σ_i} and S_{T_i} are stress coefficients related

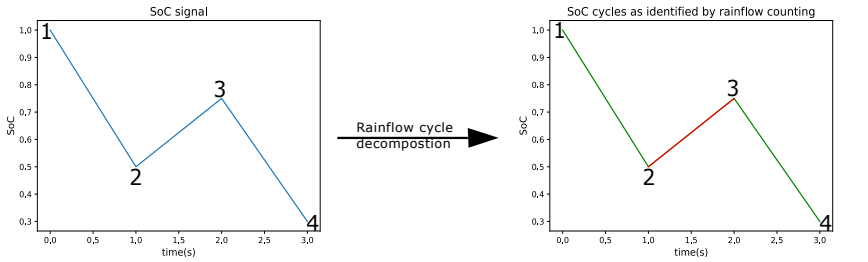

Cycle	w	σ	δ
1-4	1	0.65	0.7
2-3	0.5	0.6	0.2

Figure 2: Rainflow-Counting applied to a simple SoC(t). The amplitude σ, mean δ and w are represented for the 2 cycles identified.

respectively DoD, mSoC and temperature. These stress coefficients are determined empirically, and the chosen functions, adapted from the work in [43], are described by:

$$\begin{aligned} S_{\sigma_i} &= e^{k_\sigma(\sigma_i - \sigma_{ref})} \\ S_{T_i} &= e^{k_T(T_i - Tref)\frac{T_{ref}}{T}} \\ S_{\delta_i} &= (k_{\delta_1}\delta_i^{k_{\delta_2}} + k_{\delta_3})^{-1} \end{aligned} \tag{24}$$

The terms k_σ, k_T, k_{δ_1}, k_{δ_2} and k_{δ_3} are constants determined empirically by experiments, while σ_{ref} and T_{ref} are experimental reference values for mSoC and temperature, respectively. The temperature T_i is taken as the average temperature of cycle i, which, in this work, is assumed to be normally distributed around the temperature that should be guaranteed by the battery management system.

Finally, $\Delta SoH(X_z, v_{max}, a_{max})$ can be expressed as:

$$\Delta SoH(X_z, v_{max_z}, a_{max_z}) = SoH_0 - SoH(t, X_z, v_{max_z}, a_{max_z}) \tag{25}$$

where SoH_0 is the SoH before performing a mission plan, considered to be known in advance.

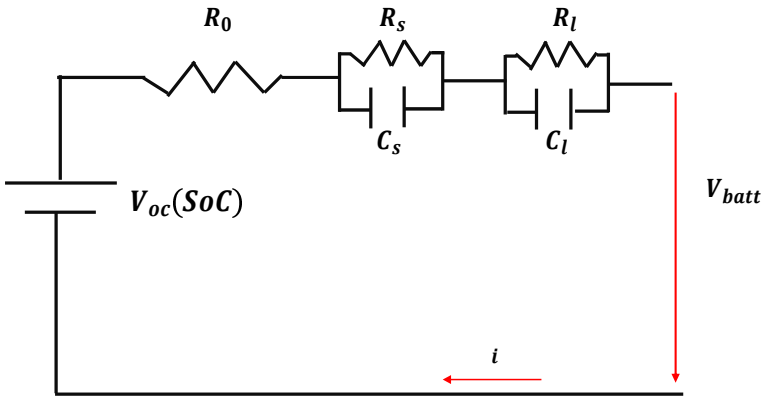

Figure 3: Second-order ECM for a battery.

4.2. SoC estimation method

To obtain the stress factors used in the degradation model, it is necessary to estimate the $SoC(t)$, which is also a used as a constraint in the EVRP-DVP. To do so, vehicle's longitudinal dynamics are combined with the second-order Equivalent Circuit Model (ECM) shown in Figure 3 that represents the internal dynamics of the battery.

The resulting system of algebraic and differential equations, given decision variables X_z, v_{max_z} and a_{max_z} is:

$$\dot{v} = a(t, X_z, v_{max_z}, a_{max_z}) \tag{26}$$

$$P_{mec}(t) = \frac{\rho_{air} C_w A v(t)^3}{2} + mgv(t)\sin\alpha + mgC_r v(t)\cos\alpha + ma(t)v(t) \tag{27}$$

$$P_{elec}(t) = \frac{P_{mec}(t)}{\eta(v(t), a(t))} \tag{28}$$

$$I(t) = \frac{1}{2R_o}(V_{OC}(SoC(t)) - V_l(t) - V_s(t) - \sqrt{(V_{OC}(SoC(t)) - V_l(t) - V_s(t))^2 - 4R_o P_{elec}(t)}) \tag{29}$$

$$\dot{V}_s = -\frac{V_s}{R_s C_s} + \frac{I(t)}{C_s} \tag{30}$$

$$\dot{V}_l = -\frac{V_l}{R_l C_l} + \frac{I(t)}{C_l} \tag{31}$$

$$\dot{SoC} = -\frac{I(t)}{Q_0} \tag{32}$$

Equation (26) relates the speed $v(t)$ and the acceleration $a(t, X_z, v_{max_z}, a_{max_z})$ which is the acceleration performed by a vehicle z following the mission plan defined by X_z with maximum speed and maximum acceleration limited to v_{max_z} and a_{max_z}.

Equation (27) describes the mechanical power based on the longitudinal dynamics of a vehicle, m is the total mass of the vehicle, which will depend on decision variables w_{ij}, g is the gravity acceleration, α is the instantaneous road inclination, C_r is the rolling resistance coefficient, C_w is the drag coefficient, A is the frontal area of the vehicle and ρ_{air} is the air density.

Equations (29 -32) are derived from the second-order ECM. $V_{batt}(t)$ is the voltage of the battery, $I(t)$ is the instantaneous current, $V_s(t)$ and $V_l(t)$ are electric potential differences with R_0, R_s, R_l being the resistances, C_l and C_s are the capacitors and $V_{OC}(SoC(t))$ is the open circuit voltage which depends on SoC.

$V_{OC}(SoC)$ can be determined with look-up tables usually provided by battery suppliers, and therefore, this system can be solved knowing the initial values of v, V_s, V_l, SoC and the function $a(t, X_z, v_{max_z}, a_{max_z})$.

4.3. Acceleration model

Solving the system of algebraic numerical equations that describes SoC, requires modeling $a(t, X_z, v_{max_z}, a_{max_z})$. To avoid relying on large amounts of data, we adopt a method similar to the one used in [8]. It based on the road information such as maximum allowed speed, inclination and traffic lights locations, to infer how acceleration will evolve. The first step of this method is to use all the aforementioned road information to create a road graph $G_r = (N_r, E_r)$. The nodes of this graph represent points in the map in which the necessary parameters to estimate the mechanical power (Equation 27) change or stops are expected (traffic lights, steep curves and etc). The edges of this graph, $e_r \in E_r$, are referred to as *road links* and can be described by:

$$e_r = \begin{bmatrix} len \\ v_{road}^{max} \\ \alpha \\ Stop \\ Curve \end{bmatrix} \tag{33}$$

where len is the road link length, α is its inclination, v_{road}^{max} its maximum allowed speed , and $Stop$ is a binary variable that is equal 1 if there is a possible stop at the end of the link (crossroad and traffic lights, as mentioned) and 0 otherwise. Similarly, the binary variable $Curve$ indicates if there is a curve at the end e_r. Figure 4 illustrate the process of building G_r based on road information.

Once G_r is built, acceleration can be estimated with assumptions over driver behaviour on each e_r. It is assumed that a vehicle z will accelerate constantly, with acceleration a_{max_z} until reaching a target speed v_{tgt}:

$$v_{tgt} = \min[v_{max}^{road}, v_{max_z}] \tag{34}$$

showing the impact of decision variables v_{max_z} and a_{max_z} on how $a(t, X_z, v_{max_z}, a_{max_z})$ is inferred. If there is a stop at the end of a road link, vehicles are considered to

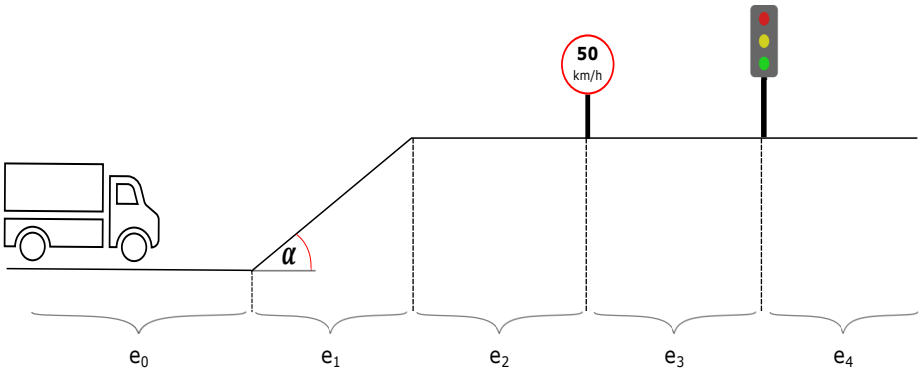

Figure 4: Example of how road links are defined. In this example, four links are shown. Links are created to represent differences on the parameters relevant to acceleration or power estimation. In this example, e_1 and e_2 are created due to a inclination difference with respect to the previous link. e_3 is defined due to a maximum speed change and e_4 is defined due to the presence of a traffic light.

break before reaching its end. Figure 5 shows the considered acceleration and speeds for a basic case in which the vehicle starts at idle and there is a Stop at the end of the link.

To obtain acceptable results in practical applications, it is necessary to consider corner cases. In [8], two such cases were considered. The first one happens when there is a difference of target speed between two consecutive road links. If the target speed in the first link is higher than in the second, the vehicle needs to decelerate before entering the second link. This is illustrated in Figure 6.The second case happens when a road link is not long enough for the vehicle to reach v_{tgt}, as shown in Figure 7.

In this paper, a third case is considered. Originally, in [8], steep curves were considered as stops. In order to be less conservative and also consider the effect of less steep curves on the speed, we account for curves assuming that vehicles will make turns with constant centripetal acceleration and therefore, their speeds before the curve will be:

$$v_{curve} = \sqrt{a_{centripetal} r} \tag{35}$$

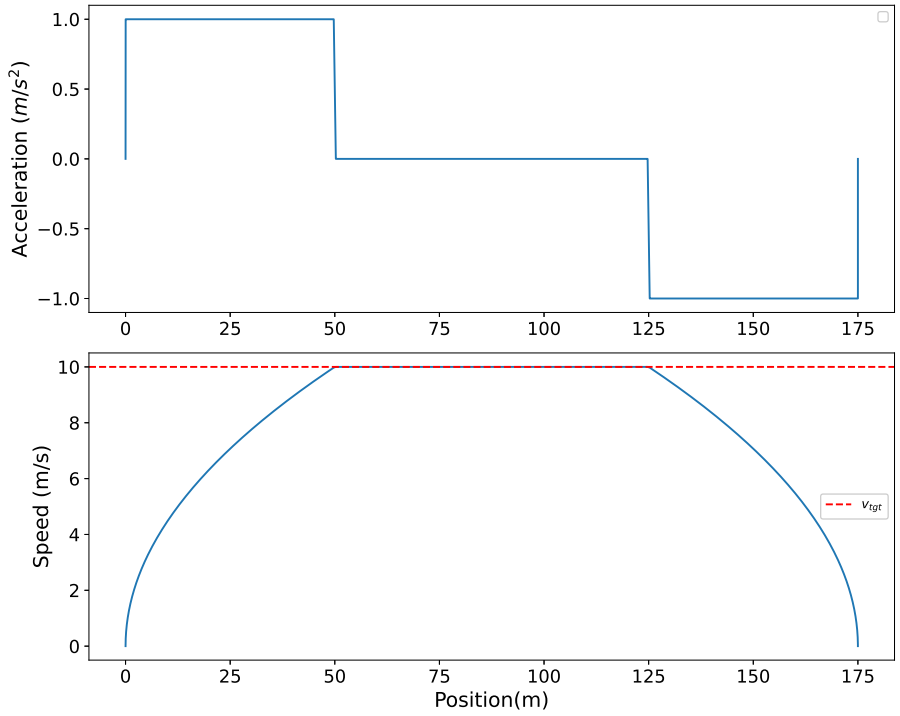

Figure 5: Vehicle speed starting at idle and going through a road link with a stop at its end.

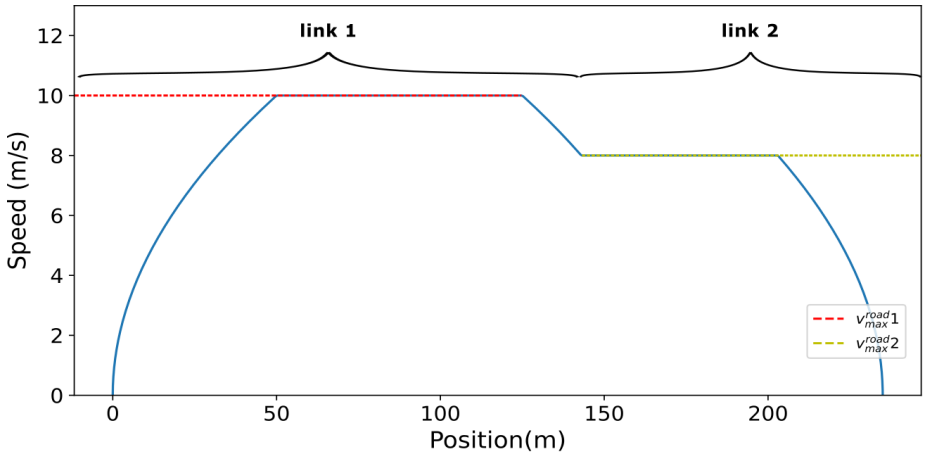

Figure 6: Speed with vehicle travelling through two consecutive road links.

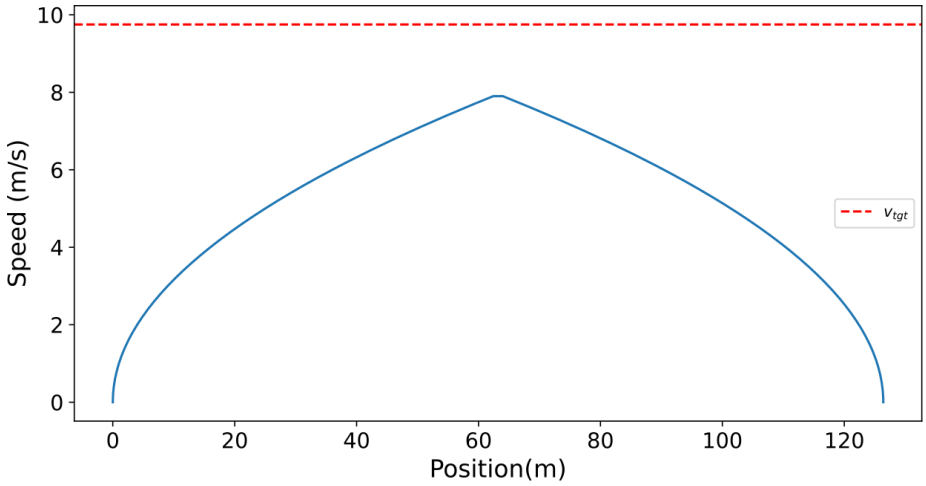

Figure 7: Speed in a short link with stop point at beginning and end. The vehicle cannot reach target speed.

with $a_{centripetal}$ being the vehicles centripetal acceleration which is considered constant among road links. The r curve radius curve can be estimated with the road information mentioned.

It is important to highlight that, even considering those corner cases, this driving model is simplified. In reality, driving behaviour can be unpredictable and more complex, for example, in eco-driving trained drivers tend to accelerate smoothly and keep steady speeds around optimal values (not necessarily maximum road speed) [19, 3]. However, as seen in [8] this method is suitable for decision-making problems and achieved good in terms of energy estimation when compared with real data. Once $a(t, X_z, v_{max_z}, a_{max_z})$ is estimated, it is possible to solve the system and obtain $SoC(t, X_z, v_{max_z}, a_{max_z})$ given the decision variables of the EVRP-DVP and estimate the SoH evolution.

4.4. Charging model

To model SoC while charging, an approach similar to the one adopted in [30] is used. SoC is considered to evolve according to a piece-wise linear function as shown in Figure 8 and charging SoC is therefore fully determined by f_{iz} and

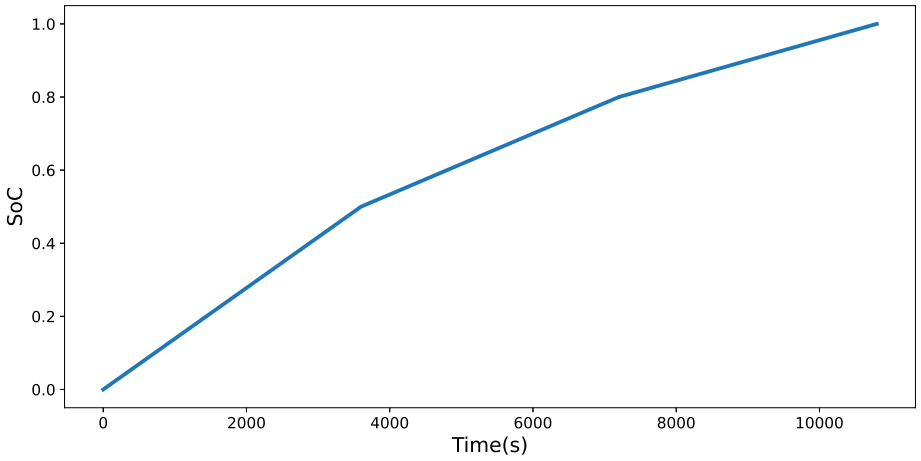

Figure 8: Non-linear charging process approximated by a piece-wise linear function.

the SoC level at which the vehicle has arrived at a charging station, which can in turn be estimated as described in the previous section.

5. Optimization Algorithm

The main drawback of the optimization model proposed is the computational burden of evaluating a possible solution. This comes from the need to solve a differential equation system and from the fact that the Rainflow-Counting decomposition has no closed form and is non-linear [36].

To solve the problem, an heuristic optimization method should then be used. Genetic programming techniques are chosen since they can be successfully used for computationally expensive optimization problems [38] and have already been employed in vehicle routing problems [25, 23].

The solution representation contains 4 parts: a mission plan π, a set of maximum speeds v_{max}, a set of maximum accelerations a_{max} and a set of recharge times f.

Figure 9 presents an example of solution for a case with 2 EV's. Vehicle 1 goes from node A0 to B3, then to E4 and so on. Its speed is limited to 60 km/h and its acceleration to 1 m/s^2. Similarly, Vehicle 2 goes from A0 to C5 and so

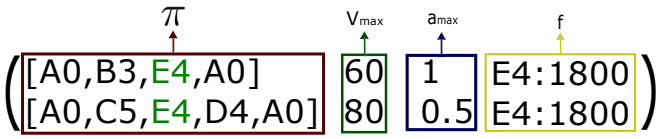

Figure 9: Solution representation.

on, with a speed limited to 80 km/h and a maximum acceleration of 0.5 m/s^2. Both of them will recharge their batteries for 1800 seconds in recharge station $E4$.

To initialize the algorithm, random solutions are created. The mission plan is created by choosing a permutation of the client nodes C and then randomly adding recharge stations between clients. The HQ is put at the beginning and end of the mission plan. This ensures that constraints (7) to (10) are respected. After that, for each recharge station in the plan, a recharge time is randomly generated, creating the recharge times set f.

Each part of the representation undergoes crossover separately and the operators used were variations of classical ones, such as order based and one-point crossover for the mission part and uniform sampling crossover for speed, acceleration and recharge parts.

Mutations of the mission plans consisted of swapping missions for a given truck; For the remaining parts small deviations were randomly added. Those processes also accounted for the constraints of the problem, not allowing for mission configurations or scalar values that would not respect the constraints of the problem.

To account for constraint 18, the fitness function has a penalization factor. Solutions that do not ensure acceptable SoC levels are penalized, being allowed to generate offspring and explore the limits of the constraints, but are highly unlikely to be selected as a final solution.

6. Results and Discussions

6.1. SoC and SoH model inclusion benefits

The proposed degradation model requires a physics based SoC model capable of capturing the internal dynamics of the battery. This model introduces computational complexities for solving EVRPs, therefore, in this section, a series of numerical experiments is performed to justify and show the differences between our approach to SoC and the most common literature model. The following model is used as a benchmark:

$$v(t) = v_{max}^{road} \tag{36}$$

$$P_{mec}(t) = \frac{\rho_{air} C_w A v(t)^3}{2} + mgv(t)\sin\alpha + mgC_r v(t)\cos\alpha \tag{37}$$

$$P_{elec}(t) = \frac{P_{mec}(t)}{\eta} \tag{38}$$

$$I(t) = \frac{P_{elec}(t)}{V_{batt}^{nominal}} \tag{39}$$

$$\dot{SoC} = -\frac{I(t)}{Q_0} \tag{40}$$

Equations 36, 37 and 38 represent the very common approach of neglecting acceleration effects and considering that vehicles always drive at road maximum speed [18]. η is a constant efficiency. Equations 39 and 40 represent the common approach of considering battery terminal voltage constant and equals to its nominal value $V_{batt}^{nominal}$.

In the first experiment, shown in Figure 10, the effects of considering battery dynamics on different electrical quantities are explored. In this experiment, a constant electrical power input is applied to the battery, representing an idealized case in which a vehicle constantly drives with a low steady speed. The power value was chosen to represent a heavy vehicle in low speed (approximately 10 km/h) and for both models, batteries were considered to have a 41 Ah capacity and were fully discharged. With this constant power, the benchmark model considers that terminal voltage and current remain constant since it neglects

Quantity	MSE	Final error
Current (A)	0.08	.21
Terminal Voltage (V)	0.29	-0.7
SoC	0.014	-
Depletion time (h)	-	1.8

Table 2: Summary of numerical experiment dedicated to compare the performance of the proposed model with classical literature approaches. Mean Squared Error (MSE) was computed in the horizon in which both batteries haven't reached full depletion. Final error represents the difference between the two models when depletion is reached. As can be seen, the benchmark model tends to be more optimistic and fails to capture changes on battery operation.

battery dynamics. In our approach, in contrast, the different electrical quantities are considered to change through time. As a consequence, SoC obtained by both models is significantly different and battery depletion is considered to happen approximately 1.8 hours later by the benchmark model. This difference is already relevant in long-haul applications and can be even more relevant for different power inputs. The summary of the experiment is found in Table 2.

While the first experiment illustrates differences caused only by considering the internal dynamics of the battery, a second experiment was designed to showcase the effects of assumptions around vehicle speeds. Figure 11 shows the differences between position, speed and SoC as considered by both model. As can be seen, speeds are significantly different for both models. Since in this displacement vehicles drive through road links that are not long enough to reach target speed, acceleration and brakes have non neglectable effects on speed. As a consequence, the duration of the displacement $t_{displacement}$ is different according to both models. This can have serious consequences when dealing with optimization models whose constraints are based on mission deadlines. Furthermore, ignoring acceleration effects when estimating power causes significant differences on SoC estimations. Even for a relatively small displacement of 25 km, the difference in SoC is already 2%. Once again, for longer displacements, this can lead to optimization solutions which are not feasible, since the bench-

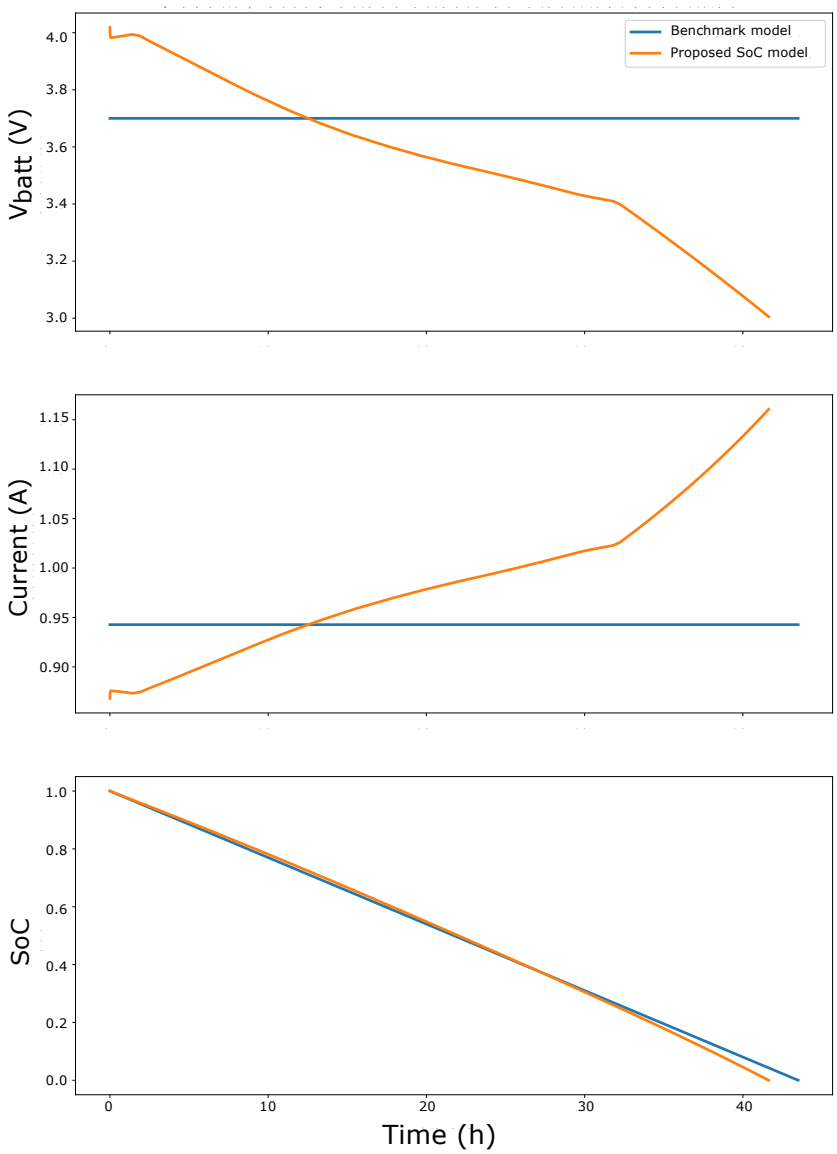

Figure 10: Modeling assumption effects on electrical quantities.

mark model tends to be more optimistic.

Both experiments highlight the importance of more realistic SoC models from the point of view of range limitation and displacement duration. In a third numerical experiment, we also show how important precise SoC modeling is for long-term degradation estimation. Two SoC estimation methods are used for the displacement represented in Figure 12. The duration of 6 of those displacements is equivalent to a working day, referred to as work cycle. SoH is estimated using the model presented in Section 4.1 considering as input SoC estimated with the benchmark model and with our approach. Figure 13 shows the comparison of SoH estimates after each cycle.

The error introduced by SoC estimation gives a significant SoH difference in the long-term. Since each cycle is equivalent to a working day, the estimation difference was of approximately six months, which justifies the used of a more realistic SoC models in long-term applications.

6.2. Results on a synthetic map

A series of numerical experiments were performed in order to assess the impact of considering degradation in routing problems. The first set of experiments was conducted in a synthetic network shown in Figure 15.

The vehicle and battery parameters used are shown in Table 3. They were either taken from the literature [42] or inferred from models used in the Volvo Group.

6.2.1. Influence of considering degradation

In the first set of experiments, different instances of the EVRP-DVP were solved with different cost parameters to investigate how taking degradation into account impacted the mission plan. When a instance is solved considering $c_{batt} = 0$ we obtain a classic EVRP where energy consumption is minimized. When $c_e = 0$ the EVRP will minimize only degradation, ignoring energy consumption. Finally having $c_{batt} \neq 0$ and $c_e \neq 0$ we have the complete EVRP-DVP.

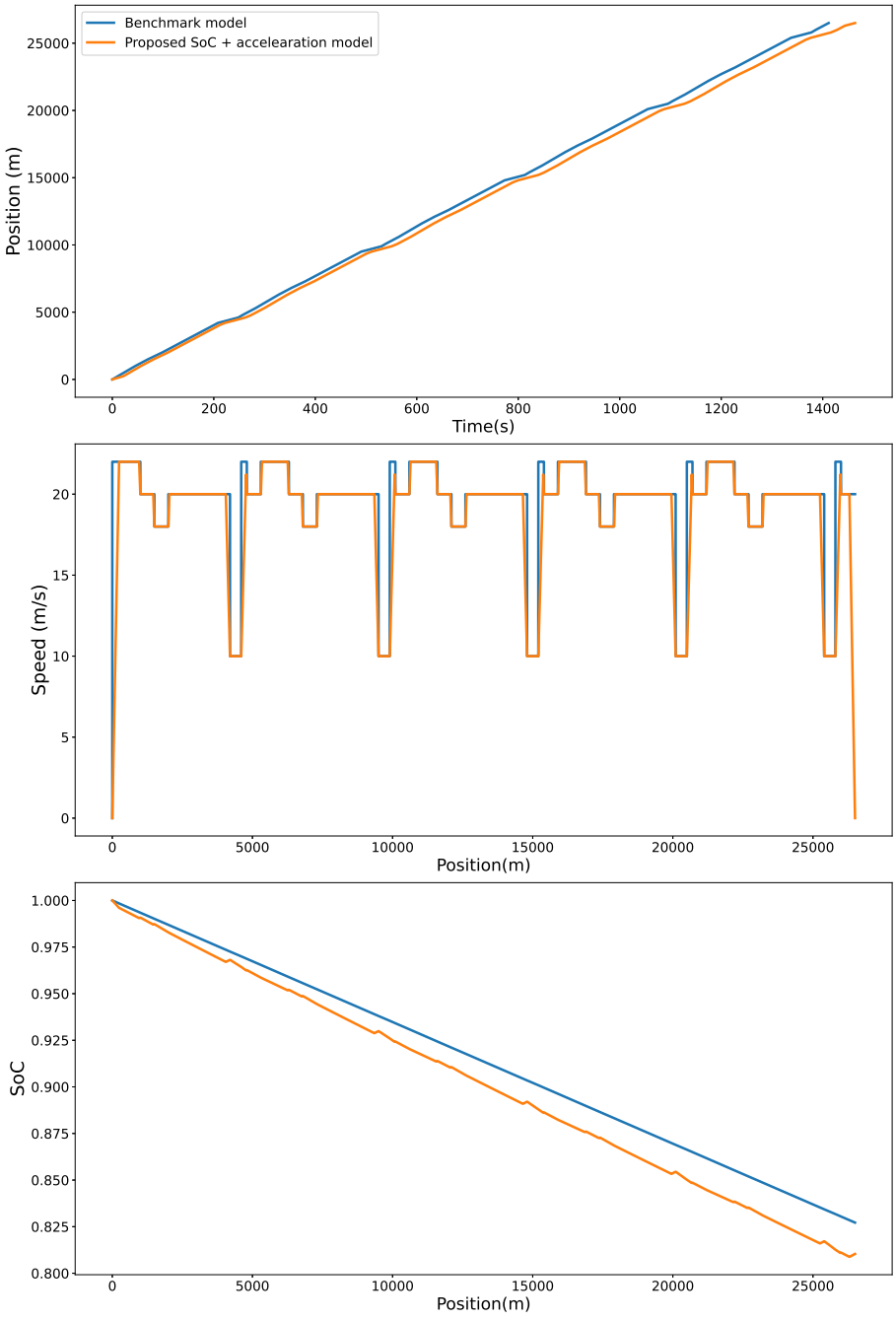

Figure 11: Comparison between position, speed and SoC as estimated by the two different models

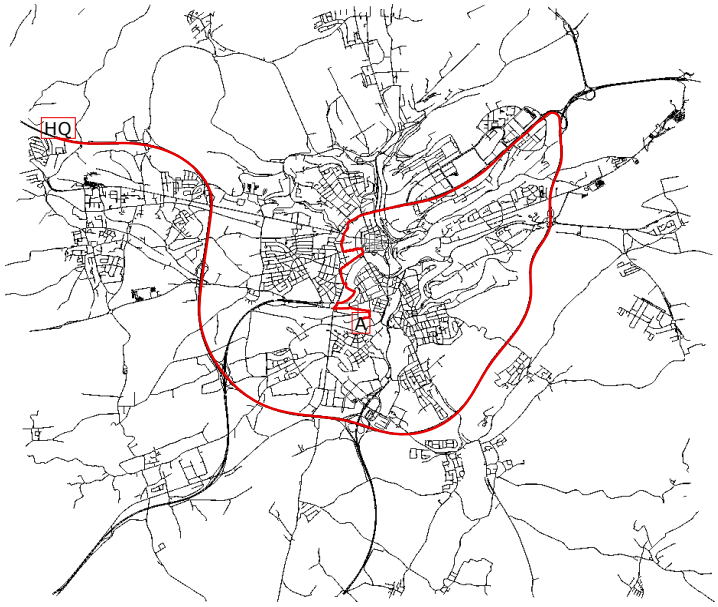

Figure 12: Illustration of the displacement used in the SoC Estimation comparison. The map is a SUMO grid model of Luxembourg, containing real topography information. The red line indicates vehicle trajectory while HQ indicates the starting point and A indicating the arrival address.

Parameter	**Value**
m	10700 (kg)
SoC_0	1
C_s	1498.26 (F)
R_s	0.01902(Ω)
C_l	120 (F)
R_l	0.02221 (Ω)
R_0	0.03417(Ω)
C_0	65453.28 (F)

Table 3: Simulation parameters

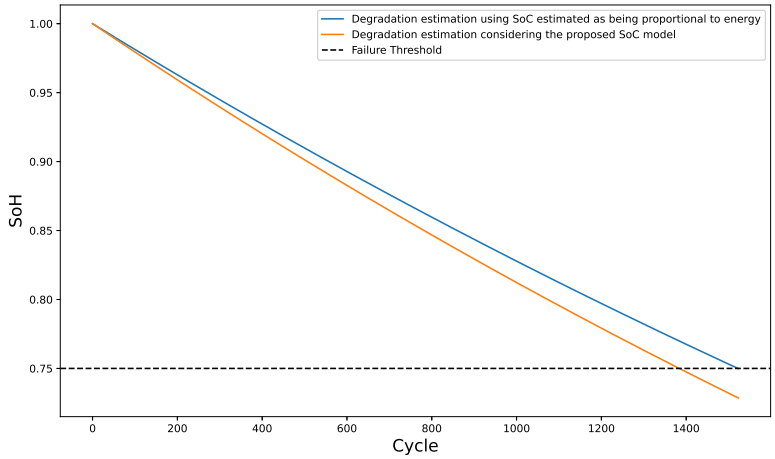

Figure 13: Comparison of end of life estimation : accurate SoC model vs. SoC variation as directly proportional to the traveled distance.

The results are reported in Table 4. It is possible to see that accounting for degradation ($c_{batt} \neq 0$) impacts the mission plan. Plans that account for degradation either have extra recharges or make charges at different moments. Most of these charges are not strictly necessary from the point of view of respecting constraint (16). They are included to reduce degradation by introducing less damaging cycles, with a lower DoD. This is clearly illustrated by Figure 14 which shows the SoC evolution obtained following the optimal mission plans obtained for the same instance, but for different optimization cases: accounting for both degradation and energy ($c_{batt} \neq 0$ and $c_e \neq 0$), for energy only ($c_{batt} = 0$) or for degradation only ($c_e = 0$).

- When only energy is considered (*i.e.* $c_{batt} = 0$), no charge is planned. This solution reduces the energy cost by minimizing displacements and stops. However, it generates cycles that are more damaging.
- When only degradation is considered (*i.e.* $c_e = 0$), two charges take place, inducing smaller cycles and causing less degradation. Since vehicles need

Instance	c_{batt} (€)	c_d (€)	c_e (€)	**Mission plan**	**Cost C** (€)
1	10000	1	0.18	A0, E0, $E1^*$, E3, D5, A4, A2, A0	8.60
1	0	1	0.18	A0, E0, E3, D5, A4, A2, A0	8.63
1	10000	1	0	A0, E0, $E1^*$, E3, $D4^*$, D5,A4, A2, A0	8.62
2	10000	1	0.18	A0, E0, $E1^*$, E3, E5, A4, A2, A0	9.55
2	0	1	0.18	A0, E0, E3, E5, A4, A2, A0	9.60
2	10000	1	0	A0, E0, $E1^*$, E3, E5, $D4^*$, A4, A2, A0	9.57
3	10000	1	0.18	A0, B1, C5, F5, F2, $D2^*$, A2, A0	9.56
3	0	1	0.18	A0, B1, C5, F5, F2, A2, A0	10.52
3	10000	1	0	A0, B1, C5, F5, F2, $D2^*$, A2, $A1^*$, A0	9.58
4	10000	1	0.18	A0, B1, B3, $D3^*$, F3, C0, A0	7.65
4	0	1	0.18	A0, B1, B3, F3, C0, A0	7.73
4	10000	1	0	A0, B1, B3, $D3^*$, F3, $C1^*$, C0, A0	7.68

Table 4: EVRP result when considering different costs for 4 instances. Recharge stations are indicated with a $*$ and $A0$ is the headquarters in all instances. Each instance is solved three times with different c_{batt}, c_e. These solutions are then evaluated with $c_{batt} = 10000$, $c_d = 1$ and $c_e = 0.18$ to compare the advantages of considering degradation in EVRP's

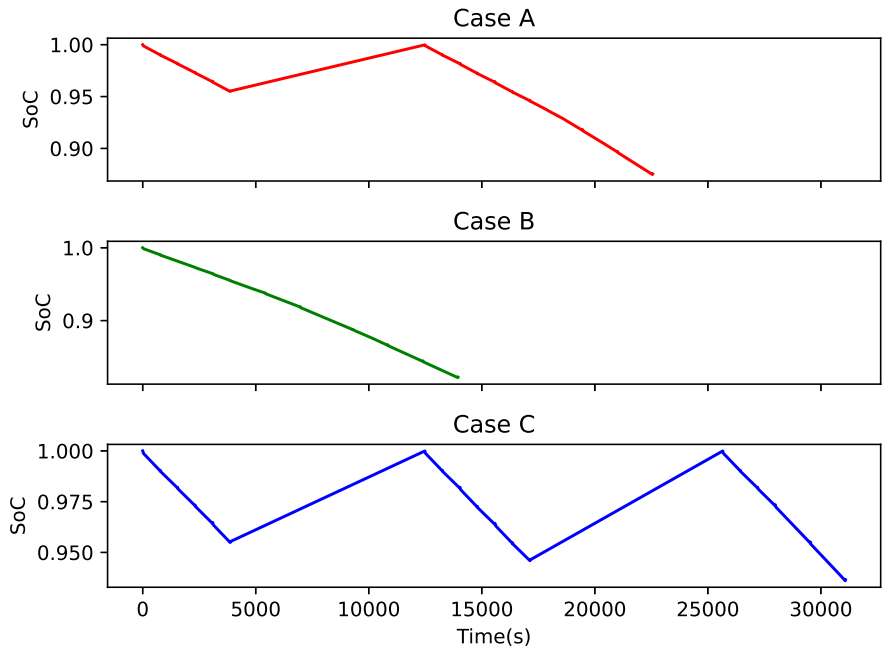

Figure 14: Comparison of SoC for optimal mission plan for different optimization cases: Case A accounts for both degradation and energy ($c_{batt} \neq 0$ and $c_e \neq 0$), case B only for energy ($c_{batt} = 0$) and case C only for degradation ($c_e = 0$).

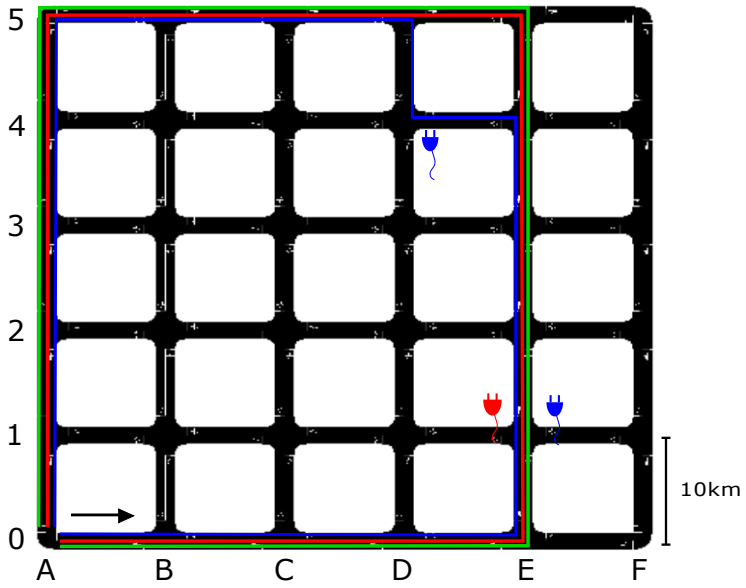

Figure 15: Different routes for instance 1 of the EVRP-DVP. Power plugs represent charges. The solutions for the case where only degradation is considered is represented in blue, in green the solution accounting only for energy consumption and in red the complete solution. The arrow indicates the sense the vehicles travelled.

to stop at charging stations to recharge, extra charging sessions result in higher energy consumption, making this solution sub-optimal from the energy point of view when compared to the case $c_e \neq 0$.

- Finally, by jointly taking into account costs of degradation and energy (*i.e.* $c_{batt} \neq 0$ and $c_e \neq 0$), a third solution is obtained. Only one charge is planned, finding a balance between extra energy consumption and degradation reduction. Figure 15 shows these three different solutions on the map.

In instance 3, considering degradation led to a 10% improvement in costs when comparing with the solution that accounted only for energy consumption. Even for instances where the improvement was more modest, because SoH evolves slowly through time, a small reduction on the cost C could lead to a huge improvement on the duration of battery life.

Clients #	**Charging stations** #	**Improvement ratio**
5	1	0.05
5	10	0.8
5	20	1
10	1	0.1
10	10	0.85
10	20	1

Table 5: Proportion of instances in which accounting for degradation yielded a better solution than only considering energy for different numbers of clients and charging stations.

6.2.2. Influence of charging stations availability

Considering degradation can impact a mission plan and improve the performance of the fleet in the long run, but some considerations must be made. Adding extra charges to reduce degradation is only beneficial when the energy consumed due to this extra stop is not significant when compared to the degradation cost. Therefore, charging station availability plays an important role on degradation minimization.

To quantify this phenomenon, random instances of the problem were generated. Each instance is solved twice, once considering only energy ($c_{deg} = 0$) and a second time considering both degradation and energy. Several instances were generated for different numbers of clients and charging stations. The proportion of instances in which considering degradation improved the solution is registered in Table 5. The column *Improvement ratio* indicates the ratio between instances in which considering degradation yielded to a better solution and those for which minimizing energy and degradation was equivalent.

As expected, the availability of charging stations plays an important role in the EVRP-DVP, allowing degradation reduction.

Another important consideration is that the optimal plan also depends on the battery dynamics and the parameters of the degradation model. Therefore,

Clients #	**Charging stations** #	**Cost** C (**not** acting on VPs)	**Cost** C (acting on VPs)
5	7	6.90	6.39
5	8	7.20	6.74
10	10	11.3	10.6
5	10	6.83	6.27
3	7	4.83	4.36

Table 6: Comparison of the impact of including Vehicle Parameters (VPs) on the average cost C

different types of batteries can result in different mission plans that will be more or less impacted by degradation.

6.2.3. Influence of vehicle driving parameters

A second set of experiments is performed to determine the importance of limiting speeds and accelerations. In these experiments, different instances are randomly generated and solved with and without limitation on speeds and accelerations. The cost parameters are $c_d = 1$, $c_e = 0.18$, $c_{batt} = 10000$.

As it can be seen in Table 6, limiting speeds and accelerations reduces the total cost of a mission plan. The decrease comes mainly from the energy cost, which is a direct consequence of equation (28), but also from the degradation cost, since stress cycles presented a smaller DoD (which can be seen in Figure 16).

In the case where speeds and accelerations are limited (Case A in Figure 16), the SoC decrease more slowly as a reflex of smaller energy consumption. Charges happened with SoC at 86% and 94% . In case Case B, where VP's are not affected, charges happened at 82% and 93%, leading to more damaging cycles. Affecting vehicle parameters can thus improve the overall efficiency of a vehicle within a mission plan, reducing both degradation and energy costs.

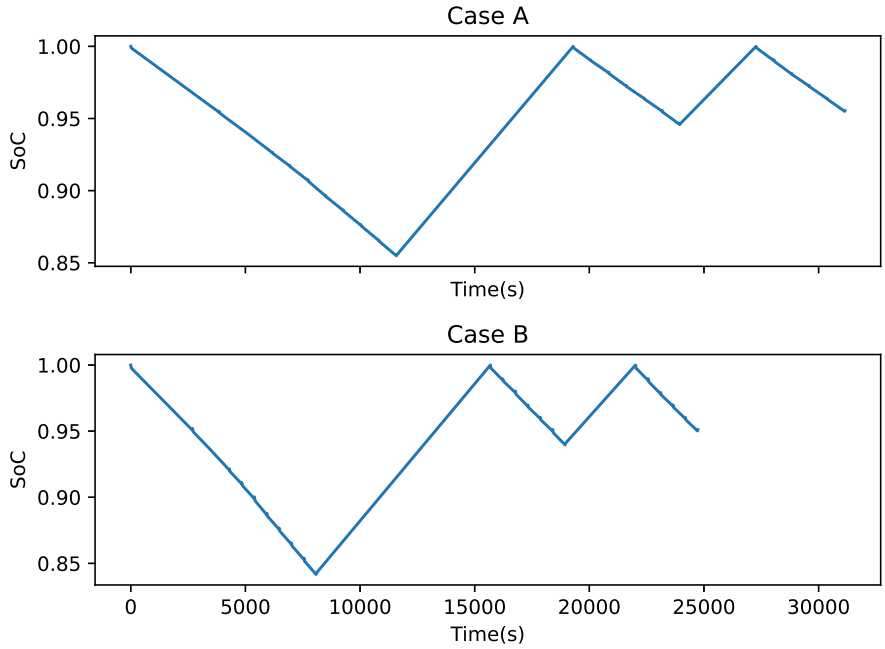

Figure 16: Comparison of SoC for optimal mission plan. Case A: acting on driving parameters, Case B: not acting on driving parameters. Notice that in Case B, the mission plan ends earlier because of different driving parameters (higher speed and acceleration)

Clients #	**Charging stations** #	**Average cost not** considering degradation	**Average cost** considering degradation
10	2	2.25	2.20
10	5	2.16	2.08
20	5	3.73	3.67
20	10	3.82	3.64
30	10	5.01	4.73
30	15	4.95	4.67

Table 7: Comparison between average cost of solutions found considering degradation and solutions without accounting for degradation.

6.3. Results on a realistic Use Case

To assess the impact of incorporating degradation in more realistic scenarios, different instances of the routing problems were generated in the map of Luxembourg, shown in Figure 12.

Instances were created choosing a specific number of random points in the map that are either charging stations or clients. As in the synthetic network experiments, they are solved once considering c_{bat} to be zero and once with $c_{bat} \neq 0$.

Table 7 shows the comparison between the results obtained with or without accounting for battery degradation. Like in the synthetic network, accounting for degradation led to better solutions. This is related to the fact that charges are planned optimally, leading to stress cycles that are less damaging. As it can be seen, the benefits are related to the number of charging stations, since charging to reduce degradation may lead to bigger energy consumption and will only occur if displacements to arrive at charging stations are relatively small.

To assess the impact of maximum speed and acceleration in realistic cases, another set of experiments is made. Instances are generated and solved with and without maximum speed and accelerations as decision variables.

Clients #	**Charging stations** #	**Average cost** **not** affecting driving parameters	**Average cost** affecting driving parameters
10	2	2.32	2.16
10	5	2.26	2.12
20	5	3.68	3.47
20	10	3.64	3.42
30	10	4.97	4.81
30	15	4.92	4.79

Table 8: Comparison between average cost of solutions found affecting driving parameters and solutions without affecting driving parameters

The results are shown in Table 8. As it can be seen, limiting speed and acceleration is beneficial in terms of cost. This is related to the fact that it reduces energy consumption which in turn is also beneficial from a degradation point of view.

7. Conclusion

This paper presented a variation of the EVRP that accounts for degradation and limitation on speeds and accelerations. To make it useful for degradation minimization in realistic scenarios, the optimization model is built upon a realistic SoC estimation method.

Since both the degradation and SoC models are computationally challenging to incorporate in optimization problems, a genetic algorithm was used to solve it.

Trough numerical experiments, the importance of realistic SoC modeling, degradation-aware decision-making and limiting speeds and accelerations is shown. Incorporating degradation and extending the set of possible actions of the problem yields to better solutions than the most usual optimization models. In real life applications this can have a beneficial impact since it can extend the useful

life of vehicles and reduce the long-term exploitation cost.

This work focused on introducing a more realistic SoH model combined with a physics based SoC model and adding it to a new EVRP variation. There are different promising research paths for future works. For example, from an optimization point of view, the performance of the proposed GAs could be studied and exact algorithms could be proposed. From a problem formulation point of view, it is necessary to compare the proposed models with real vehicle data, for SoC and SOH calibration. Incorporating stochastic elements is also desirable. For example, traffic randomness can highly affect energy consumption and delays and must, therefore, be accounted for. Long-term routing strategies and relevant aspects related to circularity such as obsolescence issues and second life applications are also interesting paths for future research.

References

[1] Khaled S Abdallah and Yasmin Adel. Electric vehicles routing problem with variable speed and time windows. In *International Conference on Industry, Engineering & Management Systems*, pages 55–65, 2020.

[2] Anagnostopoulou Afroditi, Maria Boile, Sotirios Theofanis, Eleftherios Sdoukopoulos, and Dimitrios Margaritis. Electric vehicle routing problem with industry constraints: trends and insights for future research. *Transportation Research Procedia*, 3:452–459, 2014.

[3] Cindie Andrieu and Guillaume Saint Pierre. Comparing effects of eco-driving training and simple advices on driving behavior. *Procedia-Social and Behavioral Sciences*, 54:211–220, 2012.

[4] Reza Rouhi Ardeshiri, Bharat Balagopal, Amro Alsabbagh, Chengbin Ma, and Mo-Yuen Chow. Machine learning approaches in battery management systems: State of the art: Remaining useful life and fault detection. In *2020 2nd IEEE International Conference on Industrial Electronics for Sustainable Energy Systems (IESES)*, volume 1, pages 61–66. IEEE, 2020.

[5] Issam Baghdadi, Olivier Briat, Jean-Yves Delétage, Philippe Gyan, and Jean-Michel Vinassa. Lithium battery aging model based on dakin's degradation approach. *Journal of Power Sources*, 325:273–285, 2016.

[6] John Barco, Andres Guerra, Luis Munoz, and Nicanor Quijano. Optimal routing and scheduling of charge for electric vehicles: A case study. *Mathematical Problems in Engineering*, 2017, 2013.

[7] Anthony Barré, Benjamin Deguilhem, Sébastien Grolleau, Mathias Gérard, Frédéric Suard, and Delphine Riu. A review on lithium-ion battery ageing mechanisms and estimations for automotive applications. *Journal of Power Sources*, 241:680–689, 2013.

[8] Rafael Basso, Balázs Kulcsár, Bo Egardt, Peter Lindroth, and Ivan Sanchez-Diaz. Energy consumption estimation integrated into the electric vehicle routing problem. *Transportation Research Part D: Transport and Environment*, 69:141–167, 2019.

[9] Alberto Ceselli, Ángel Felipe, M Teresa Ortuño, Giovanni Righini, and Gregorio Tirado. A branch-and-cut-and-price algorithm for the electric vehicle routing problem with multiple technologies. In *Operations Research Forum*, volume 2, pages 1–33. Springer, 2021.

[10] The European Commission. Communication from the commission - the european green deal. Technical Report COM(2019) 640, The European Commission, 2019.

[11] Emrah Demir, Katy Huckle, Aris Syntetos, Andrew Lahy, and Mike Wilson. Vehicle routing problem: Past and future. In *Contemporary operations and logistics*, pages 97–117. Springer, 2019.

[12] Stephen D Downing and DF Socie. Simple rainflow counting algorithms. *International journal of fatigue*, 4(1):31–40, 1982.

[13] Tomislav Erdelić and Tonči Carić. A survey on the electric vehicle routing problem: variants and solution approaches. *Journal of Advanced Transportation*, 2019, 2019.

[14] G Ferro, M Paolucci, and M Robba. An optimization model for electrical vehicles routing with time of use energy pricing and partial recharging. *IFAC-PapersOnLine*, 51(9):212–217, 2018.

[15] Aurélien Froger, Jorge E Mendoza, Ola Jabali, and Gilbert Laporte. Improved formulations and algorithmic components for the electric vehicle routing problem with nonlinear charging functions. *Computers & Operations Research*, 104:256–294, 2019.

[16] Daniel Gebbran, Jeppe Rich, and Tomislav Dragicevic. Electrical vehicle fleet routing accounting for dynamic battery degradation. *arXiv preprint arXiv:2203.04642*, 2022.

[17] Dominik Goeke. Granular tabu search for the pickup and delivery problem with time windows and electric vehicles. *European Journal of Operational Research*, 278(3):821–836, 2019.

[18] Dominik Goeke and Michael Schneider. Routing a mixed fleet of electric and conventional vehicles. *European Journal of Operational Research*, 245(1):81–99, 2015.

[19] Yuhan Huang, Elvin CY Ng, John L Zhou, Nic C Surawski, Edward FC Chan, and Guang Hong. Eco-driving technology for sustainable road transport: A review. *Renewable and Sustainable Energy Reviews*, 93:596–609, 2018.

[20] Raci Berk İslim and Bülent Çatay. The effect of battery degradation on the route optimization of electric vehicles. *Procedia Computer Science*, 204:1–8, 2022.

[21] Guang Jin, David E Matthews, and Zhongbao Zhou. A bayesian framework for on-line degradation assessment and residual life prediction of secondary

batteries inspacecraft. *Reliability Engineering & System Safety*, 113:7–20, 2013.

[22] Marcus Johnen, Christian Schmitz, Maria Kateri, and Udo Kamps. Fitting lifetime distributions to interval censored cyclic-aging data of lithium-ion batteries. *Computers & Industrial Engineering*, 143:106418, 2020.

[23] Sašo Karakatič. Optimizing nonlinear charging times of electric vehicle routing with genetic algorithm. *Expert Systems with Applications*, 164:114039, 2021.

[24] Ilker Kucukoglu, Reginald Dewil, and Dirk Cattrysse. The electric vehicle routing problem and its variations: A literature review. *Computers & Industrial Engineering*, 161:107650, 2021.

[25] Hui-Chieh Li, Chung-Cheng Lu, Timo Eccarius, and Min-Yi Hsieh. Genetic algorithm with an event-based simulator for solving the fleet allocation problem in an electric vehicle sharing system. *Asian Transport Studies*, 8:100060, 2022.

[26] Pedro Dias Longhitano, Khaoula Tidriri, Christophe Bérenguer, and Benjamin Echard. Joint optimization of routes and driving parameters for battery degradation management in electric vehicles. *IFAC-PapersOnLine*, 55(6):557–562, 2022.

[27] Bingshan Ma, Dawei Hu, Xiqiong Chen, Yin Wang, and Xue Wu. The vehicle routing problem with speed optimization for shared autonomous electric vehicles service. *Computers & Industrial Engineering*, 161:107614, 2021.

[28] M Amine Masmoudi, Leandro C Coelho, and Emrah Demir. Plug-in hybrid electric refuse vehicle routing problem for waste collection. *Transportation Research Part E: Logistics and Transportation Review*, 166:102875, 2022.

[29] George S Misyris, Antonios Marinopoulos, Dimitrios I Doukas, Tomas Tengnér, and Dimitris P Labridis. On battery state estimation algorithms

for electric ship applications. *Electric Power Systems Research*, 151:115–124, 2017.

[30] Alejandro Montoya, Christelle Guéret, Jorge E Mendoza, and Juan G Villegas. The electric vehicle routing problem with nonlinear charging function. *Transportation Research Part B: Methodological*, 103:87–110, 2017.

[31] Simon EJ O'Kane, Weilong Ai, Ganesh Madabattula, Diego Alonso-Alvarez, Robert Timms, Valentin Sulzer, Jacqueline Sophie Edge, Billy Wu, Gregory J Offer, and Monica Marinescu. Lithium-ion battery degradation: how to model it. *Physical Chemistry Chemical Physics*, 24(13):7909–7922, 2022.

[32] Samuel Pelletier, Ola Jabali, and Gilbert Laporte. Charge scheduling for electric freight vehicles. *Transportation Research Part B: Methodological*, 115:246–269, 2018.

[33] Samuel Pelletier, Ola Jabali, Gilbert Laporte, and Marco Veneroni. Battery degradation and behaviour for electric vehicles: Review and numerical analyses of several models. *Transportation Research Part B: Methodological*, 103:158–187, 2017.

[34] Theresia Perger and Hans Auer. Energy efficient route planning for electric vehicles with special consideration of the topography and battery lifetime. *Energy Efficiency*, 13(8):1705–1726, 2020.

[35] Roberto Roberti and Min Wen. The electric traveling salesman problem with time windows. *Transportation Research Part E: Logistics and Transportation Review*, 89:32–52, 2016.

[36] David M Rosewater, David A Copp, Tu A Nguyen, Raymond H Byrne, and Surya Santoso. Battery energy storage models for optimal control. *IEEE Access*, 7:178357–178391, 2019.

[37] Michael Schneider, Andreas Stenger, and Dominik Goeke. The electric vehicle-routing problem with time windows and recharging stations. *Transportation science*, 48(4):500–520, 2014.

[38] Yoel Tenne and Chi-Keong Goh. *Computational intelligence in expensive optimization problems*, volume 2. Springer Science & Business Media, 2010.

[39] Paolo Toth and Daniele Vigo. An overview of vehicle routing problems. *The vehicle routing problem*, pages 1–26, 2002.

[40] Jiaolong Wang, Fode Zhang, Jianchuan Zhang, Wen Liu, and Kuang Zhou. A flexible rul prediction method based on poly-cell lstm with applications to lithium battery data. *Reliability Engineering & System Safety*, 231:108976, 2023.

[41] Shunli Wang, Siyu Jin, Dekui Bai, Yongcun Fan, Haotian Shi, and Carlos Fernandez. A critical review of improved deep learning methods for the remaining useful life prediction of lithium-ion batteries. *Energy Reports*, 7:5562–5574, 2021.

[42] Bizhong Xia, Wenhui Zheng, Ruifeng Zhang, Zizhou Lao, and Zhen Sun. A novel observer for lithium-ion battery state of charge estimation in electric vehicles based on a second-order equivalent circuit model. *Energies*, 10(8):1150, 2017.

[43] Bolun Xu, Alexandre Oudalov, Andreas Ulbig, Göran Andersson, and Daniel S Kirschen. Modeling of lithium-ion battery degradation for cell life assessment. *IEEE Transactions on Smart Grid*, 9(2):1131–1140, 2016.

[44] Min Xu, Ting Wu, and Zhijia Tan. Electric vehicle fleet size for carsharing services considering on-demand charging strategy and battery degradation. *Transportation Research Part C: Emerging Technologies*, 127:103146, 2021.

[45] Hongqian Zhao, Zheng Chen, Xing Shu, Jiangwei Shen, Zhenzhen Lei, and Yuanjian Zhang. State of health estimation for lithium-ion batteries based

on hybrid attention and deep learning. *Reliability Engineering & System Safety*, 232:109066, 2023.

[46] Yu Zhou, Qiang Meng, and Ghim Ping Ong. Electric bus charging scheduling for a single public transport route considering nonlinear charging profile and battery degradation effect. *Transportation Research Part B: Methodological*, 159:49–75, 2022.

[47] Xiaorong Zuo, Yiyong Xiao, Meng You, Ikou Kaku, and Yuchun Xu. A new formulation of the electric vehicle routing problem with time windows considering concave nonlinear charging function. *Journal of Cleaner Production*, 236:117687, 2019.